R. Kovacevic and Y. M. Zhang, "Neurofuzzy model-based weld fusion state estimation," IEEE Control Systems Magazine, 17(2): 30-42, 1997.

NEUROFUZZY MODEL- BASED WELD FUSION STATE ESTIMATION

Radovan Kovacevic and Yu M. Zhang

Proper fusion is crucial in generating a sound weld. Successful control of the fusion state requires accurate measurements of both the top-side and back-side bead widths. A top-side sensor based system is preferred so that the sensor can be attached to and moved with the torch. Thus, the system must be capable of estimating the back-side bead width with high accuracy. Because skilled human operators can estimate the fusion state from the observed weld pool, a neurofuzzy system is developed to infer the back-side bead width from the pool geometry in this work. It is found that the back-side bead width can be estimated with satisfactory accuracy by the identified neurofuzzy model. Thus, accurate feedback of the fusion state can be provided for its control.

INTRODUCTION

Fusion is the primary requirement of a welding operation. The fusion state can be specified using the outline of the cross-sectional solidified weld bead. Extraction and control of the fusion outline is evidently impractical. The fusion state should be characterized by a few geometrical parameters which can easily be controlled to achieve the desired fusion.

The authors are with the Welding Research and Development Laboratory, Center for Robotics and Manufacturing Systems, University of Kentucky, Lexington, KY 40506. Email: kovacev@engr.uky.edu, yzhang01@ukcc.uky.edu.
This paper was partially presented at the 1996 IEEE International Symposium on Intelligent Control in Dearborn, MI, September 15-18, 1996. The work was supported by the National Science Foundation (DMI-9412637 and DMI-9419530) and Allison Engine Company, Indianapolis, IN.

The final goal is to control the fusion state of fully penetrated welds in gas tungsten arc (GTA) welding. The fusion state on a cross section is characterized using two parameters, the top-side and back-side widths of the fusion zone (Fig. 1). Therefore, the top-side width w and back-side bead width w_b of the weld pool are together defined as the fusion state. A multivariable system will be developed to control w and w_b.

Pool width control has been extensively studied. One of the pioneering works was done by Vroman and Brandt [1] who used a line scanner to detect the weld pool region. Chin et al. found that the slope of the infrared intensity becomes zero when the liquid-solid interface of the weld pool is crossed [2, 3]. This zero slope is caused by the emissivity difference between the liquid and solid [2]. In order to directly observe the weld pool, the intensive arc light should be avoided or eliminated. Richardson et al. proposed the co-axial observation to avoid the arc light [4]. Pietrzak and Packer have developed a weld pool width control system based on the co-axial observation [5].

The use of the pool width in welding process control is based on assuming that the pool width can characterize the weld quality. However, no studies have sufficiently shown that an inherent correlation exists between the pool width and the primary parameters of weld quality, for example, the weld penetration. On the contrary, the pool width is often not very sensitive to variations in welding conditions or changes in welding parameters, however these variations and changes may severely alter the weld penetration [6]. In addition, an increase in either the welding current or arc length will cause the pool width to increase. However, the resultant change in the weld penetration depends on which parameter (i.e., the current or the arc length) increased. If the current increases, the weld penetration increases; but if the arc length increases,

the weld penetration tends, in general, to decrease. Hence, in this case, the width itself can not provide sufficient information about the weld penetration.

Weld penetration is a critical component of the weld quality. For the case of full penetration, the state of the weld penetration is specified by the back-side bead width w_b (Fig. 1). With a back-side sensor, w_b can be reliably measured. However, it is often required that the sensor be attached to and moved with the torch to form a so-called top-side sensor. For such a sensor, w_b is invisible. Hence, extensive studies have been done to explore the possibility of indirectly measuring w_b based on pool oscillation, infrared radiation, ultrasound, and radiography. Although many valuable results have been achieved, only a few control systems are available to quantitatively estimate and control the back-side bead width.

In addition to the back-side bead width, the top-side pool width needs to be simultaneously controlled in order to accurately control the fusion state. Hence, the fusion control is a more complicated subject than weld penetration control. Hardt et al. have simultaneously controlled the depth, which specifies the weld penetration state for the case of partial penetration, and width of the weld pool using top-side and back-side sensors [7]. To obtain a top-side sensor based control system, we have proposed estimating the back-side bead width using the sag geometry behind the weld pool [8]. Based on a detailed dynamic modeling study [9], an adaptive system has been developed to control both the top-side and back-side widths of the weld pool [10].

More instantaneous and accurate information can be acquired from the weld pool. In order to use the weld pool information in welding process control, we developed a real-time image processing algorithm to detect the weld pool boundary in a previous study [11] from the images captured by a high shutter speed camera assisted with a pulsed laser [12]. Hence, the weld pool geometry can be utilized to develop more advanced welding process control systems.

It is known that skilled operators can estimate and control the welding process based on pool observation. In this work, we will develop a neurofuzzy system for estimating the back-side bead width from the pool geometry. Then, a neurofuzzy multivariable system will be designed to control the fusion state using the top-side pool width and the estimated back-side bead width as the feedback of the fusion state.

POOL GEOMETRY

In order to describe the weld pool geometry, a few characteristic parameters must be selected. In a previous study [13], the following parametric model was proposed to model the boundary of the weld pool:

$$y_r = \pm a\, x_r^b (1 - x_r)\ (a > 0,\ 1 \geq b > 0) \tag{1}$$

where a and b are the model parameters, $(x_r,\ y_r)$ are the coordinates of the pool boundary in the normalized coordinate system ox_ry_r (Fig. 2). These normalized coordinates are calculated using the measured x, y coordinates defined in Fig. 3:

$$\begin{cases} x_r = x / L \\ y_r = y / L \end{cases} \tag{2}$$

where L is the length of the weld pool.

The boundary of the weld pool can be acquired using image processing [11]. Parameters L, a, and b can be simultaneously obtained by fitting the measured boundary to model (1). Based on the resultant model parameters, the following relative width can be calculated:

$$w_r = w / L = 2a\left[\frac{b}{1+b}\right]^b \frac{1}{1+b}. \tag{3}$$

We will use $w_r L$, rather than the measured width, as the feedback of the pool width. In the following, L and w_r will be used to characterize the geometrical impression of the weld pool for estimating another parameter of the fusion state, the back-side bead width.

NEUROFUZZY MODEL

Neurofuzzy Modeling

A fuzzy system has three major conceptual components: rule base, database, and reasoning mechanism [14]. The rule base consists of the used fuzzy IF-THEN rules. The database contains the membership functions of the fuzzy sets. The reasoning mechanism performs the inference procedure which uses the IF-THEN rules to derive a reasonable output or conclusion from the input variables. Because of the ambiguous boundaries of fuzzy sets and the rule based structure, fuzzy systems can be developed to mimic the human inference. The authors notice that the weld fusion may also be estimated using other methods. However, due to the excellence of skilled operators in estimating the welding process state, the authors expect that the performance of a fuzzy logic based estimation of the weld fusion will be excellent.

In the conventional fuzzy models, the fuzzy linguistic IF-THEN rules are primarily derived from human experience [15]. Since the fuzzy modeling takes advantage of existing human knowledge which can not be easily or directly utilized in other conventional modeling methods [14], fuzzy models have been successfully used in different areas, including manufacturing [16-19]. In these models, no systematic adjustments are made on the rules, membership functions, or reasoning mechanism according to the behavior of the fuzzy model. In general, if the fuzzy rules elicited from the operators' experience are correct, relevant, and complete [20], the resultant fuzzy model can function well. However, frequently such fuzzy rules from the operators do not

satisfy the correctness, relevance, and completeness requirements [20]; the rules may be vague and misinterpreted, or the rule base could be incomplete. In such cases, the performance of the fuzzy system can be greatly improved if systematic adjustments are made based on its behavior.

The adjustability of the rules, membership functions, and reasoning mechanism provides the fuzzy model an adaptation to the addressed problem or process. In order to adjust the parameters in the fuzzy model, various learning techniques developed in the neural network literature have been used. Thus, the term neurofuzzy modeling is used to refer to the application of algorithms developed through neural network training to identify parameters for a fuzzy model [14]. A neurofuzzy model can be defined as a fuzzy model with parameters which can be systematically adjusted using the training algorithms in neural network literature. In neurofuzzy modeling, the abstract thoughts or concepts in human reasoning are incorporated with numerical data so that the development of fuzzy models becomes more systematic and less time consuming. As a result, neurofuzzy systems have been successfully used in different areas [21-24].

Most neurofuzzy systems have been developed based on the Sugeno-type fuzzy model [25]. A typical fuzzy rule in a Sugeno-type model has the form: IF x is A and y is B THEN $z = f(x,y)$. Here A and B are fuzzy sets, and $z = f(x,y)$ is a crisp function which can be any function as long as the system outputs can be appropriately described within the fuzzy region specified by the antecedent of the rule [14]. In this paper, a neurofuzzy system will be developed to estimate the fusion state based on the Sugeno model. The resultant model will then be used in the projected neurofuzzy model based control system of the fusion state.

Neurofuzzy Model for Fusion Estimation

It is common practice to use the domain knowledge about the addressed problem or process for determining the fuzzy model structure, i.e., selecting the relevant inputs, partitioning the

fuzzy sets, etc., and numerical data for identifying the parameters in the fuzzy model [14]. We selected the length and narrowness, measured by L and w_r, as two relevant fuzzy variables for representing our impression about the geometrical characteristics of the weld pool geometry. These two variables are denoted as p_j $(j = 1,\ 2)$ where $p_1 = L$ and $p_2 = w_r$. Based on the knowledge of the welding process, we have assumed that each variable has no more than four fuzzy sets. By modeling trials it is found that two fuzzy sets are enough for each variable. Thus, the partition shown in Table 1 is obtained. The membership to A_{ji} is given by:

$$A_{ji}(p_j) = \exp\left(-\frac{(p_j - a_{ji})^2}{b_{ji}}\right) \quad (1 \le i \le I_j), \tag{4}$$

where a_{ji} and b_{ji} are the parameters of the fuzzy membership function $A_{ji}(p_j)$ which will be identified using the experimental data.

For a given set of input variables (p_1, p_2), the following rule is implemented:

$$\begin{aligned} &\text{Rule } (i_1, i_2)\text{: IF } p_1 \text{ is } A_{1i_1} \text{ and } p_2 \text{ is } A_{2i_2} \\ &\quad \text{THEN } y(i_1, i_2) = c_1(i_1, i_2)p_1 + c_2(i_1, i_2)p_2 \\ &\qquad\qquad (1 \le i_1 \le I_1,\ 1 \le i_2 \le I_2) \end{aligned} \tag{5}$$

for all possible (i_1, i_2)'s, where $c_j(i_1, i_2)'s$ are the so-called consequent parameters [21], and $y(i_1, i_2)$ is an output from rule (i_1, i_2). In a standard first-order Sugeno model [21, 14], $y(i_1, i_2)$ has the form $y(i_1, i_2) = c_0 + c_1(i_1, i_2)p_1 + c_2(i_1, i_2)p_2$. For processing convenience, the inputs and output have been normalized before the neurofuzzy model is identified (see Eq. (26)). Because of this normalization, as shown by the modeling trials, c_0's are not significant for every rule (i_1, i_2) $(1 \le i_1 \le I_1,\ 1 \le i_2 \le I_2)$. Hence, linear crisp functions as in Eq. (5) are used.

The final output of the fuzzy model is:

$$y = \sum_{i_1=1}^{I_1} \sum_{i_2=1}^{I_2} w(i_1, i_2) y(i_1, i_2) \tag{6}$$

where $w(i_1, i_2)$ is the weight representing the truth degree for the premise: p_1 is A_{1i_1} and p_2 is A_{2i_2}, and is calculated using the equation:

$$w(i_1, i_2) = \prod_{j=1}^{2} A_{ji_k}(p_j). \tag{7}$$

IDENTIFICATION ALGORITHM

The identification of a fuzzy model consists of structure identification and parameter estimation. During identification, the parameters are estimated for different structures. The final structure, i.e., the fuzzy variable partition in this case, is selected by comparing different models. This is, in general, very inefficient. Also, the decision is made purely based on statistic (mathematic) analysis. No process characteristics and designer's experience are involved. If the designer is familiar with the process, an experience-based partition may be appropriate. Thus, as suggested in [14], we have selected and partitioned the fuzzy variables based on our understanding of the welding process. Hence, the identification of the fuzzy model is simplified as a parameter estimation problem.

Denote the data as:

$$\{p_1(t), p_2(t), y(t)\} \quad (t = 1,\ 2,\ \ldots,\ N) \tag{8}$$

where N is the size of the data. Also, denote the model calculated output as

$$\hat{y}(t) = \sum_{i_1=1}^{I_1} \sum_{i_2=1}^{I_2} w(i_1, i_2;\ t) y(i_1, i_2;\ t) \quad (t = 1,\ 2,\ \ldots,\ N) \tag{9}$$

where

$$\begin{cases} w(i_1, i_2;\ t) = \prod_{j=1}^{2} A_{ji_j}(p_j(t)) \\ y(i_1, i_2;\ t) = \sum_{j=1}^{2} c_j(i_1, i_2) p_j(t) \end{cases} \quad (t = 1,\ 2,\ \ldots,\ N). \tag{10}$$

Define the cost function

$$J\{(a_{ji}, b_{ji})'s\ (1 \le i \le I_i,\ 1 \le j \le 2);\ c_j(i_1, i_2)'s\ (1 \le j \le 2,\ 1 \le i_k \le I_k,\ 1 \le k \le 2))\} = \sum_{t=1}^{N} (y(t) - \hat{y}(t))^2. \tag{11}$$

The parameter estimation is to find the optimal parameters $\{(a_{ji}^{*}, b_{ji}^{*})'s,\ c_j^{*}(i_1, i_2)'s\}$ so that

$$J\{(a_{ji}^{*}, b_{ji}^{*})'s\ ;\ c_j^{*}(i_1, i_2)'s\ \} = \min J\{(a_{ji}, b_{ji})'s\ ;\ c_j(i_1, i_2)'s\ \}. \tag{12}$$

Although many excellent algorithms such as the second-order back-propagation [26] and normalized cumulative learning rule [27] proposed in the neural network literature can be used to speed up the parameter identification, the authors found that satisfactory identification speed can be achieved by using the simplest, but the most frequently used, δ rule [27, 28] in this case. In order to implement this algorithm, partial derivatives of the cost function with respect to each of the model parameters are needed. It can be shown:

$$\frac{\partial J}{\partial a_{ji}} = -2\sum_{t=1}^{N} \delta(t) \frac{\partial \hat{y}(t)}{\partial a_{ji}} = -2\sum_{t=1}^{N} \delta(t) \sum_{i_1=1}^{I_1} \sum_{i_2=1}^{I_2} y(i_1, i_2;\ t) \frac{\partial w(i_1, i_2;\ t)}{\partial a_{ji}} = 4\sum_{t=1}^{N} \delta(t) \sum_{i_1=1}^{I_1} \sum_{i_2=1}^{I_2} \gamma(i_j - i) y(i_1, i_2;\ t) w(i_1, i_2;\ t) \frac{p_j(t) - a_{ji}}{b_{ji}} \tag{13}$$

where

$$\gamma(k) := \begin{cases} 1 & (k = 0) \\ 0 & (k \ne 0) \end{cases}, \tag{14}$$

$$\delta(t) := y(t) - \hat{y}(t). \tag{15}$$

Here the subscripts, j and i, of a_{ji} indicate the fuzzy variable (p_j) and its set i, respectively.

Similarly,

$$\frac{\partial J}{\partial b_{ji}} = -2 \sum_{t=1}^{N} \delta(t) \sum_{i_1=1}^{I_1} \sum_{i_2=1}^{I_2} y(i_1, i_2;\ t) \frac{\partial w(i_1, i_2;\ t)}{\partial b_{ji}}$$

$$= -2 \sum_{t=1}^{N} \delta(t) \sum_{i_1=1}^{I_1} \sum_{i_2=1}^{I_2} \gamma(i_j - i) y(i_1, i_2;\ t) w(i_1, i_2;\ t) \frac{(p_j(t) - a_{ji})^2}{{b_{ji}}^2}. \tag{16}$$

For the partial derivatives with respect to the consequent parameters, we have

$$\frac{\partial J}{\partial c_j(i_1, i_2)} = -2 \sum_{t=1}^{N} \delta(t) w(i_1, i_2;\ t) p_j(t). \tag{17}$$

Thus, the parameters of the fuzzy model can be estimated using the following iterative algorithm:

(0) Select initial parameters:

$$\begin{cases} (a_{ji}^{(0)}, b_{ji}^{(0)})'s \ (1 \le i \le I_j,\ 1 \le j \le 2) \\ c_k^{(0)}(i_1, i_2)'s \ (1 \le k \le 2,\ 1 \le i_j \le I_j,\ 1 \le j \le 2) \end{cases} \tag{18}$$

and let $n = 1$.

(1) For $(1 \le i_1 \le I_1,\ 1 \le i_2 \le I_2,\ 1 \le t \le N)$, calculate

$$\begin{cases} w^{(n-1)}(i_1, i_2;\ t) = \prod_{j=1}^{2} \exp\left(-\frac{(p_j(t) - a_{ji_j}^{(n-1)})^2}{b_{ji_j}^{(n-1)}} \right) \\ y^{(n-1)}(i_1, i_2;\ t) = \sum_{j=0}^{2} c_j^{(n-1)}(i_1, i_2) p_j(t) \end{cases}. \tag{19}$$

(2) For $1 \le t \le N$, calculate

$$\delta^{(n-1)}(t) = y(t) - \hat{y}^{(n-1)}(t) = y(t) - \sum_{i_1=1}^{I_1} \sum_{i_2=1}^{I_2} w^{(n-1)}(i_1, i_2;\ t) y^{(n-1)}(i_1, i_2;\ t). \tag{20}$$

(3) Calculate

$$J^{(n-1)} = \sum_{t=1}^{N} [\delta^{(n-1)}(t)]^2. \tag{21}$$

(4) For $(1 \le i \le I_j,\ 1 \le j \le 2)$, calculate

$$a_{ji}^{(n)} = a_{ji}^{(n-1)} - 4\varepsilon_1 \sum_{t=1}^{N} \delta^{(n-1)}(t) \sum_{i_1=1}^{I_1} \sum_{i_2=1}^{I_2} \gamma(i_j - i) y^{(n-1)}(i_1, i_2;\ t) w^{(n-1)}(i_1, i_2;\ t) \frac{p_j(t) - a_{ji}^{(n-1)}}{b_{ji}^{(n-1)}}, \tag{22}$$

and

$$b_{ji}^{(n)} = b_{ji}^{(n-1)} + 2\varepsilon_2 \sum_{t=1}^{N} \delta^{(n-1)}(t) \sum_{i_1=1}^{I_1} \sum_{i_2=1}^{I_2} \gamma(i_j - i) y^{(n-1)}(i_1, i_2;\ t) w^{(n-1)}(i_1, i_2;\ t) \frac{(p_j(t) - a_{ji}^{(n-1)})^2}{(b_{ji}^{(n-1)})^2}. \tag{23}$$

(5) For $(1 \le i_1 \le I_1,\ 1 \le i_2 \le I_2,\ 1 \le j \le 2)$, calculate

$$c_j^{(n)}(i_1, i_2) = c_j^{(n-1)}(i_1, i_2) + 2\varepsilon_3 \sum_{t=1}^{N} \delta^{(n-1)}(t) w^{(n-1)}(i_1, i_2;\ t) p_j(t). \tag{24}$$

(6) If $n = 1$, let $n = n + 1$ and go to (1).

(7) If $\left| J^{(n-1)} - J^{(n-2)} \right| < \boldsymbol{\varepsilon}$, go to (8). Otherwise, let $n = n + 1$ and go to (1).

(8) Let

$$\begin{cases} a_{ji}^{*} = a_{ji}^{(n)} & (1 \le i \le I_i,\ 1 \le j \le 2) \\ b_{ji}^{*} = b_{ji}^{(n)} & (1 \le i \le I_i,\ 1 \le j \le 2) \\ c_j^{*}(i_1, i_2) = c_j^{(n)}(i_1, i_2) & (1 \le i_1 \le I_1,\ 1 \le i_2 \le I_2,\ 1 \le j \le 2). \end{cases} \tag{25}$$

In the above algorithm, $\boldsymbol{\varepsilon}_j$'$s > 0$ $(j = 1,\ 2,\ 3)$ are the learning coefficients and $\boldsymbol{\varepsilon} > 0$ is the iterative accuracy control parameter. By properly selecting the initial parameters, learning coefficients, and iterative control parameter, the final estimates of the parameters in the fuzzy model can be obtained.

EXPERIMENTATION

Data set (8) for identifying the fuzzy model will be generated from experimentation. The data generation plays a critical role in guaranteeing the validity of the acquired model. The experiments must be properly designed. In particular, the experimental data should be generated so that the weld pools with different geometry are produced using different sets of welding

parameters. Consider the welding parameter vector $(i,v,l)^T$ where i, v, and l denote the welding current, torch speed, and arc length respectively. Assume the permitted ranges are $I_{\min} \le i \le I_{\max}$, $V_{\min} \le v \le V_{\max}$, and $l_{\min} \le l \le l_{\max}$. These ranges define a welding parameter vector space. For the given discrete resolutions, the vector space consists of finite points. Theoretically, welding parameters corresponding to all the points in the space should be used to generate the experimental data. However, it is known that the back-side bead width is determined by several weld pools over a time interval, rather than a single pool at an instant. If the weld pool does not change rapidly, the weld pool at an instant can be a good approximation over the interval. If the weld pool does change rapidly, the dynamics of the correlation between the back-side bead width and weld pool will have to be addressed, which greatly complicates the study. In order to avoid possible complexity, it is preferred that the welding parameters be kept constant during an experiment. However, the number of experiments would be too large. Hence, in addition to the use of some constant welding parameters, other welding parameters are programmed to slowly change during an experiment.

The experimental setup is shown in Fig. 3. In this paper, the experimental setup is used for conducting open-loop experiments using the pre-programmed welding parameters. (During closed-loop control, the welding parameters will be determined by the feedback control algorithm.) The welds are made using DCEN GTA welding. The welding current is controlled by the computer through its analog output to the power supply ranging from 10 A to 200 A. The torch and camera are attached to a 3-axial manipulator. The motion of the manipulator is controlled by the 3-axis motion control board which receives the commands from the computer. The motion can be pre-programmed and modified on-line by the computer in order to achieve the required torch speed and trajectory, including the arc length. The Control Vision's ultra-high

shutter speed vision system [12] is used to capture the weld pool images. This system consists of a strobe-illumination unit (pulse laser), camera head and system controller. The pulse duration of the laser is 3 ns, and the camera is synchronized with the laser pulse. Thus, the intensity of laser illumination during the pulse duration is much higher than those of the arc and hot metal. Using this vision system, good weld pool contrast can always be obtained under different welding conditions. In this study, the camera views the weld pool from the rear at a 45° angle. The frame grabber digitizes the video signals into 512×512 $8bit$ digital image matrices. By improving the algorithm and hardware, the weld pool boundary can now be acquired on-line in 80 ms.

Eight experiments have been done using the welding parameters illustrated in Fig. 4 on separate workpieces. The workpieces are 1 mm thick stainless steel 304 plates which are 250 mm in length and 100 mm in width. The shielding gas is pure argon. Compared with the torch speed, current, and arc length, the influence of the shielding gas rate and electrode tip angle on the welding process is relatively small. Thus, the shielding gas rate and the tip angle are kept constant (7.5 L/min. and 45°) in the experiments.

The weld pool parameters, i.e., the pool length L and relative pool width w_r, are measured on-line at 10 Hz. The back-side bead width is measured off-line at the same rate using a structured-light 3D vision algorithm developed in our previous study [29]. Fig. 5 shows the plots of the experimental outputs sampled at one second intervals.

MODELING AND DISCUSSION

Modeling

The number of parameters in the membership functions is $2(I_1 + I_2)$. The number of consequent parameters is $2I_1 I_2$. Thus, the number of parameters in fuzzy model (9) is 16 when $I_1 = 2$ and $I_2 = 2$. For such a number of parameters, too large N may not be necessary. Hence, we only use the measurements taken at integer seconds to constitute the data set (8). In addition, we have removed the data in the first 10 seconds in each experiment. Finally, a data set $\{p_1(t), p_2(t), y(t)\}$ $(t = 1,\ 2,\ \ldots,\ N)$ with $N = 670$ is obtained.

For processing convenience, the data have been normalized:

$$\begin{cases} p_j(t) \Leftarrow \dfrac{p_j(t) - \min p_j}{\max p_j - \min p_j} \quad (j = 1,\ 2), \\ y(t) \Leftarrow \dfrac{y(t) - \min y}{\max y - \min y}. \end{cases} \tag{26}$$

The normalized data range from 0 to 1. We have assigned $(a_{11}^{(0)}, a_{12}^{(0)}) = (1,\ 0)$, $(a_{21}^{(0)}, a_{22}^{(0)}) = (1,\ 0)$, $(b_{11}^{(0)}, b_{12}^{(0)}) = (0.85^2,\ 0.85^2)$, and $(b_{21}^{(0)}, b_{22}^{(0)}) = (0.85^2,\ 0.85^2)$. Once these initial partition parameters are given, the consequent parameters should be carefully assigned in order to avoid too large initial fitting errors. Analysis shows that when the parameters of the fuzzy partition are given, the correlation between the cost function and the consequent parameters are quadratic. Thus, the cost function can be analytically minimized with respect to the consequent parameters in this case. The resultant consequent parameters will be used as the initial parameters in the iterative estimation of the fuzzy model. Denote

$$\begin{cases} ii = 2(i_1 - 1)I_2 + 2(i_2 - 1) + j \\ w(ii; t) = w(i_1, i_2; t) p_j(t) \\ \boldsymbol{\theta}(ii) = c_j(i_1, i_2) \\ x(t) = (w(1; t), \ldots, w(M; t)) \\ Y = (y(1),\ y(2),\ \ldots,\ y(N))^T \\ \boldsymbol{\theta} = (\boldsymbol{\theta}(1), \ldots, \boldsymbol{\theta}(M))^T \end{cases} \tag{27}$$

where $M = 2I_1I_2$ is the number of the consequent parameters, $x(t)$ is the observation vector, and $\boldsymbol{\theta}$ is the consequent parameter vector. It can be shown that

$$\hat{y}(t) = x(t)\theta . \tag{28}$$

Thus, the least square estimate of the consequent parameter vector is

$$\hat{\boldsymbol{\theta}} = (\Phi^T\Phi)^{-1}\Phi^T Y \tag{29}$$

where

$$\Phi = (x(1)^T \ldots\ldots x(N)^T)^T . \tag{30}$$

Hence, the initials of the consequent parameters can be provided by $\hat{\boldsymbol{\theta}}$.

The values of $\boldsymbol{\varepsilon}_k > 0$ ($k = 1, 2, 3$) can be determined by calculation trials. Too large $\boldsymbol{\varepsilon}_k's > 0$ result in a non-converged iteration, whereas too small $\boldsymbol{\varepsilon}_k's > 0$ gives a slow convergence. We have used variable $\boldsymbol{\varepsilon}_k's > 0$. The initial $\boldsymbol{\varepsilon}_k's > 0$ can be relatively large. If the cost function increases, $\boldsymbol{\varepsilon}_k's > 0$ are halved. Otherwise, $\boldsymbol{\varepsilon}_k's > 0$ are not changed. Thus, both the speed and convergence of the iterative computation is guaranteed. By trials, we selected initial $\boldsymbol{\varepsilon}_1 = \boldsymbol{\varepsilon}_2 = 0.0005$ and $\boldsymbol{\varepsilon}_3 = 0.005$. The accuracy control parameter $\boldsymbol{\varepsilon} = 0.001$. Using these parameters, the resultant MatLab program can identify the fuzzy model from the data set quickly with guaranteed convergence.

The identified neurofuzzy model has the following four rules:

Rule (1, 1): IF p_1 is **long** and p_2 is **wide** THEN $y(1, 1) = 1.04p_1 + 0.31p_2$
Rule (1, 2): IF p_1 is **long** and p_2 is **narrow** THEN $y(1, 2) = 0.39p_1 + 0.015p_2$
Rule (2, 1): IF p_1 is **short** and p_2 is **wide** THEN $y(2, 1) = 0.54p_1 + 0.30p_2$
Rule (2, 2): IF p_1 is **short** and p_2 is **narrow** THEN $y(2, 2) = 0.04p_1 - 0.08p_2$

Here the variables are measured using the normalized coordinates with $\min y = 0.69$ mm, $\max y = 4.16$ mm, $\min p_1 = 3.22$ mm, $\max p_1 = 7.21$ mm, $\min p_2 = 0.62$, and $\max p_2 = 1.07$. The resultant fuzzy partition can be shown by using the membership functions in Fig. 6.

Accuracy and Comparison

The fitting accuracy of the resultant fuzzy model can be seen in Fig. 7. It is apparent that the back-side bead widths measured from different experiments, which were performed using different welding parameters, have been fitted with quite satisfactory accuracy by the fuzzy model. The maximum error is about ten percent of $(\max y - \min y)$, i.e., about 0.4 mm. No obvious static errors have been observed. The high frequency sparks can be easily removed using a proper filter. Thus, the neurofuzzy model can be used to estimate the back-side bead width based on the weld pool geometry for the fusion control.

Using the resultant fuzzy model, the weld pool geometry from the eight experiments can be used to calculate the back-side bead width in order to test the estimation accuracy of the fuzzy model. The results are shown in Fig. 8. In the calculation, all the data which were measured during welding at 10 Hz have been used. It can be seen that the test accuracy is very close to the fitting accuracy shown in Fig. 7. The maximum prediction error is also about 0.4 mm. It is known that the weld penetration is very sensitive to disturbances when the weld pool is near to the partial/full penetration border [30]. If the desired back-side bead width is too small, slight disturbances may change the weld pool from the full penetration to the partial penetration so that the resultant welds are unacceptable. In order to guarantee the full penetration, the desired back-side bead width should be at least 2 mm. Under this assumption, 1 mm is an acceptable maximum error. If the prediction error does not exceed 0.5 mm, the prediction accuracy can be regarded as quite satisfactory. Hence, Fig. 8 shows that an satisfactory estimation can be

expected from the resultant fuzzy model. This excellence will be further shown through the on-line estimation experiments later.

In order to explore the possible accuracy improvement, we have used $I_1 = I_2 = 3$ and $I_1 = I_2 = 4$. However, no noticeable improvement has been observed regarding the maximum error and overall impression. Fig. 9 shows the case of $I_1 = I_2 = 3$. The fitting results are very close to Fig. 7. The cost function is 1.17, whereas the cost function is 1.26 when $I_1 = I_2 = 2$. It is evident that the partition of the two fuzzy sets in Table 1 is sufficient.

To justify the use of the fuzzy model, a linear model has also been fitted. The resultant equation is:

$$w_b = 0.86L + 0.36w_r \tag{31}$$

where all of the parameters are measured using their normalized coordinates (Eq. (26)). The resultant cost function is 2.81. This number is much larger than the cost function of the fuzzy model. Fig. 10 illustrates the fitting results using the linear model (31). Substantial static fitting errors can be frequently observed. It is apparent that the fuzzy model does provide much better estimates of the back-side bead widths.

Fuzzy Knowledge

The identified fuzzy model can reveal the roles the weld pool parameters play in determining the weld penetration. Based on these rules, the following knowledge can be inferred:

(1). Rule (1, 1) and Rule (2, 1) show that the influence of the narrowness of the weld pool on w_b almost does not depend on the length of the weld pool when the weld pool is wide.

(2). The influence of the length of the weld pool on w_b always depends on the narrowness of the weld pool, despite the length of the weld pool. In particular, when the pool is long, the partial derivative of w_b with respect to L changes from 0.39 to 1.04 when the pool becomes wide (Rule

(1, 2) and Rule (1, 1)). When the pool is short, this partial derivative increases from 0.04 to 0.54 when the pool becomes wide (Rule (2, 2) and Rule (2, 1)).

(3) When the pool is short and narrow, the sensitivity of w_b, which specifies the state of the full penetration, to the changes in both the length and narrowness are low (Rule (2, 2)). However, it should be pointed that this low sensitivity is observed in the case of full penetration. Beyond the range of full penetration, this observation may not be true. In fact, it has been found that the weld penetration is sensitive to the welding parameters when the weld is nearly penetrated [30]. Thus, when the weld pool is nearly penetrated, a small increase in the inputted heat could cause the weld pool to penetrate. Once the weld pool is penetrated, the sensitivity of the penetration increase will become less sensitive to the increased heat input.

In order to illustrate the above observations, Fig. 11 plots the resultant neurofuzzy model using parametric curves. From these parametric curves, the partial derivative curves shown in Fig. 12 can be obtained. It is clear that the deviation of $\partial w_b / \partial w_r$ curves with respect to the length is very pronounced when the pool is narrow (Fig. 12(b)). This deviation becomes much smaller when the pool becomes wide (Fig. 12(b)). Thus, the influence of the narrowness of the weld pool on w_b does not significantly depend on the length when the pool is wide, whereas it does when the pool is narrow. For $\partial w_b / \partial L$ (Fig. 12(a)), its dependence on w_r can always be observed over the whole range of the pool length, although this dependence slightly decays when w_r increases. The low sensitivities of w_b to the changes in both the length and narrowness can also be seen from the curve with parameter $w_r = 0.6$ at $L = 3$ mm in Fig. 12(a) and the curve with $L = 3$ mm at $w_r = 0.6$ in Fig. 12(b), respectively.

It is apparent that the above observations provide us knowledge about the correlation between the weld penetration (w_b) and weld pool geometry. They are derived from the neurofuzzy

model. If a linear model is used, the correlation acquired between the weld penetration and weld pool geometrical parameters will only be an average over the entire range of the weld pool geometrical parameters. The above observations can not be drawn. Hence, the fuzzy modeling plays an important role in deriving the detailed correlation between the weld penetration, therefore the fusion state, and the weld pool geometry.

ON-LINE ESTIMATION

An on-line calculation of the resultant neurofuzzy model can be done in less than 4 ms on a 90 MHz Pentium processor. Hence, the feedback of the fusion state can be provided in real-time. Figs. 13-14 show two on-line estimation experiments. The material, plate thickness, workpiece dimensions, rate of shielding gas, and angle of the electrode tip are the same as those used in the experiments for data generation.

In Experiment 1, the current range is [40A, 60A] (Fig. 13a). The resultant top-side parameters are shown in Fig. 13(b). In the experiments for generating identification data, the welding parameters have been designed so that the resultant back-side bead width (state of the full penetration) falls within the permitted range. However, the welding current in the present experiment significantly exceeds the range used in generating the identification data. As a result, very long weld pools, compared with the pools in the experiments for identification data generation (Fig. 5), are frequently observed (Fig. 13b). Excessive full penetration is therefore produced. The back-side bead width often exceeds the permitted maximum (Fig. 13c). For our application, the estimation accuracy for such an extreme range is not required. In the permitted penetration, say $1 \text{ mm} \leq w_b \leq 4 \text{ mm}$ range, the prediction made by the neurofuzzy model is quite

accurate. Hence, the developed neurofuzzy model can be used to estimate the back-side bead width for the fusion state control.

The welding current range in Experiment 2 is reduced to [40A, 50A] (Fig. 14a). Although the resultant pool length is beyond the range in Fig. 5, the excessiveness of the pool length and back-side bead width (Fig. 14b and c) is not severe. Hence, accurate on-line prediction has been made by the neurofuzzy model. This again shows that the developed neurofuzzy model can estimate the fusion state with sufficient accuracy.

CONCLUSIONS

The fusion state can be described by the top-side width and back-side width of the weld pool in the case of full penetration. Fusion control therefore implies both the control of the top-side weld size as well as weld penetration. The fitted model of the pool boundary directly provides the top-side weld size. Using the developed neurofuzzy system, the weld penetration state can be estimated with good accuracy from the pool geometry. Hence, the feedback of the fusion state is achieved. In addition, the fuzzy modeling plays an important role in deriving the detailed correlation between the weld penetration and the weld pool geometry.

ACKNOWLEDGMENT

The assistance of Mr. Lin Li in conducting this research is greatly appreciated.

REFERENCES

[1] A. R. Vorman, and H. Brandt, “Feedback control of GTA welding using puddle width measurement,” *Welding Journal*, vol. 55, no. 9, pp. 742-749, 1976.

[2] W. Chen, and B. A. Chin, “Monitoring joint penetration using infrared sensing techniques,” *Welding Journal*, vol. 69, no. 4, pp. 181s-185s, 1990.

[3] P. Banerjee, et al., “Infrared sensing for on-line weld geometry monitoring and control,” *ASME Journal of Engineering for Industry*, vol. 117, no. 3, pp. 323-330, 1995.

[4] R. W. Richardson, et al., “Coaxial arc weld pool viewing for process monitoring and control,” *Welding Journal*, vol. 63, no. 3, pp. 43-50, 1984.

[5] K. A. Pietrzak, and S. M. Packer, “Vision-based weld pool width control,” *ASME Journal of Engineering for Industry*, vol. 116, no. 1, pp. 86-92, 1994.

[6] Y. M. Zhang, R. Kovacevic, and L. Wu, “Sensitivity of torch-side weld geometry in representing the full penetration,” Proc. Instn. Mech. Engrs., Part. B: *Journal of Engineering Manufacture*, vol. 206, no. 3, pp. 191-197, 1992.

[7] J.-B. Song and D. E. Hardt, “Dynamic modeling and adaptive control of the gas metal arc welding process,” *ASME Journal of Dynamic Systems, Measurement, and Control,* vol. 116, no. 3, pp. 405-413, 1994.

[8] Y. M. Zhang, et al., “Determining joint penetration in GTAW with vision sensing of weld-face geometry,” *Welding Journal*, vol. 72, no. 10, pp. 463s-469s, 1993.

[9] Y. M. Zhang, R. Kovacevic, and L. Wu, “Dynamic analysis and identification of gas tungsten arc welding process for full penetration control,” *ASME Journal of Engineering for Industry,* vol. 118, no. 1, pp. 123-136, 1996.

[10] Y. M. Zhang, R. Kovacevic, and L. Li, “Adaptive control of full penetration gas tungsten arc welding,” *IEEE Transactions on Control Systems Technology,* vol. 4, no. 4, pp. 394-403, 1996.

[11] R. Kovacevic, Y. M. Zhang, and R. Ruan, “Sensing and control of weld pool geometry for automated GTA welding,” *ASME Journal of Engineering for Industry,* vol. 117, no. 2, pp. 210-222, 1995.

[12] T. Hoffman, “Real-time imaging for process control,” *Advanced Material & Processes*, vol. 140, no. 3, pp. 37-43, 1991.

[13] Y. M. Zhang, L. Li, and R. Kovacevic, “"Dynamic estimation of full penetration using geometry of adjacent weld pools," to appear in *ASME Journal of Manufacturing Science and Engineering* (formerly *Journal of Engineering for Industry*) , vol. 119, no. 2, 1997.

[14] J. S. R. Jang and C. T. Sun, “Neuro-fuzzy logic modeling and control,” *Proceedings of the IEEE,* vol. 83, no. 3, pp. 378-406, 1995.

[15] E. H. Mamdani and S. Assilian, “An experiment in linguistic synthesis with a fuzzy logic controller,” *International Journal of Machine Studies,* vol. 7, no. 1, pp. 1-13, 1975.

[16] R. Du, M. A. Elbestawi, and S. M. Wu, "Automated monitoring of manufacturing processes, part 1: monitoring methods," *ASME Journal of Engineering for Industry,* vol. 117, no. 2, pp. 121-132, 1995.

[17] T. J. Ko, and D. W. Cho, "Tool wear monitoring in diamond turning by fuzzy pattern recognition," *ASME Journal of Engineering for Industry,* vol. 116, no. 2, pp. 225-232, 1994.

[18] S. B. Billatos and J. A. Webster, "Knowledge-based expert system for ballscrew grinding," *ASME Journal of Engineering for Industry,* vol. 115, no. 2, pp. 239-235, 1993.

[19] X. D. Fang, "Expert system-supported fuzzy diagnosis finish-turning process states," *International Journal of Machine Tools and Manufacture,* vol. 35, no. 66, pp. 913-924, 1995.

[20] M. Brown and C. Harris, *Neurofuzzy adaptive modeling and control,* Prentice Hall, New York, 1994.

[21] K. Tanaka, M. Sano, and H. Watanabe, "Modeling and control of carbon monoxide concentration using a neuro-fuzzy technique," *IEEE Transactions on Fuzzy Systems,* vol. 3, no. 3, pp. 271-279, 1995.

[22] K. Hayashi, et al., "Neuro fuzzy transmission control for automobile with variable loads," *IEEE Transactions on Control Systems Technology,* vol. 3, no. 1, pp. 49-53, 1995.

[23] A. M. Sharaf, and T. T. Lie, "Neuro-fuzzy hybrid power system stabilizer," *Electric Power Systems Research,* vol. 30, no. 1, pp. 17-23, 1994.

[24] O. S. Mesina and R. Langari, "Neuro-fuzzy system for tool condition monitoring in metal cutting," in *Dynamic Systems and Control*, Vol. 2, pp. 931-938, 1994 ASME International Mechanical Engineering Congress, ASME, 1994.

[25] T. Takagi and M. Sugeno, "Fuzzy identification of systems and its applications to modeling and control," *IEEE Transactions on Systems, Man, and Cybernetics,* vol. 15, no. 1, pp. 116-132, 1985.

[26] D. B. Parker, "Optimal algorithms for adaptive networks: second order back propagation, second order direct propagation, and second order {H}ebbian learning," *Proceedings of IEEE International Conference on Neural Networks,* pp. 593-600, 1987.

[27] *Using NeuralWorks.* NeuralWare, Inc., Pittsburgh, PA, 1993.

[28] S. Haykin, *Neural networks: a comprehensive foundation,* Macmillan College Publishing Company, New York, 1994.

[29] Y. M. Zhang and R. Kovacevic, “Real-time sensing of sag geometry during GTA welding,” *ASME Journal of Manufacturing Science and Engineering* (formerly *Journal of Engineering for Industry*)*,* vol. 119, no. 1, Feb. 1997.

[30] P. Burgardt and C. R. Heiple, “Weld penetration sensitivity to welding variables when near full joint penetration,” *Welding Journal*, vol. 71, no. 9, pp. 341s-347s, 1992.

BIOGRAPHY

Radovan Kovacevic:

Radovan Kovacevic received the B.S. and M.S. degrees in mechanical engineering from the University of Belgrade, Yugoslavia, 1n 1969 and 1972, respectively, and the Ph.D. degree in mechanical engineering from the University of Montenegro, Podgorica, Yugoslavia, in 1978.

He joined the faculty of the Department of Mechanical Engineering at the University of Kentucky, Lexington, Kentucky in January 1991 and was promoted to Full Professor in May of 1995. He was an Associate Professor of Mechanical Engineering at Syracuse University, Syracuse, NY (1987-1990), and, for more than 16 years, was a faculty member at the University of Montenegro, Podgorica, Yugoslavia. He is the Director of the Laboratory for Advanced Manufacturing Processes, Welding Research and Development Laboratory, and Machine Vision and Neural Networks Laboratory at the Center for Robotics and Manufacturing Systems. His research includes physics of traditional and advance manufacturing processes and welding processes; and machine vision in quality control. He has published more than 200 technical papers, four books, and holds two U. S. patents.

Dr. Kovacevic is an Honorary Consultant Professor at the Harbin Institute of Technology, Harbin, China. He, together with Dr. Yu M. Zhang, is the recipient of The Donald Julius Groen Prize 1995 awarded by The Institution of Mechanical Engineers, England.

Yu M. Zhang:

Yu M. Zhang received the B.S. and M.S. degrees in control engineering, and the Ph.D. degree in mechanical engineering, all from Harbin Institute of Technology (HIT), China, in 1882, 1984, and 1990, respectively.

He joined the National Key Laboratory for Advanced Welding Production Technology at HIT in 1984 as a Junior Lecturer, and was promoted to Professor in 1993. Since 1991, he has been with Center for Robotics and Manufacturing Systems at the University of Kentucky, Lexington, Kentucky, as a Research Fellow and has assisted Prof. R. Kovacevic develop an active welding and industrial application program. He holds one U. S. patent and is the author/co-author of over 50 journal papers and one book. His research and development field covers industrial automation, modeling, monitoring and control of manufacturing processes, machine vision, and adaptive/robust/neurofuzzy/predictive control systems.

Dr. Zhang, with Prof. R. Kovacevic, is the recipient of The Donald Julius Groen Prize 1995 awarded by The Institution of Mechanical Engineers, England.

LIST OF ILLUSTRATIONS AND TABLE

Table 1 Partition of Fuzzy Input Variables

Fuzzy variables	Number of Fuzzy Sets	Partition
length (p_1)	$I_1 = 2$	long (A_{11}), short (A_{12})
narrowness (p_2)	$I_2 = 2$	wide (A_{21}), narrow (A_{22})

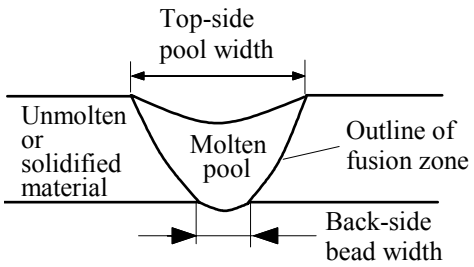

Fig. 1 Fusion parameters of fully penetrated weld pool.

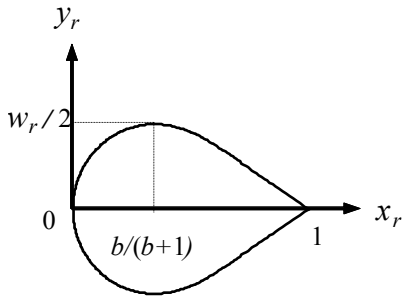

Fig. 2 Normalized coordinate system.

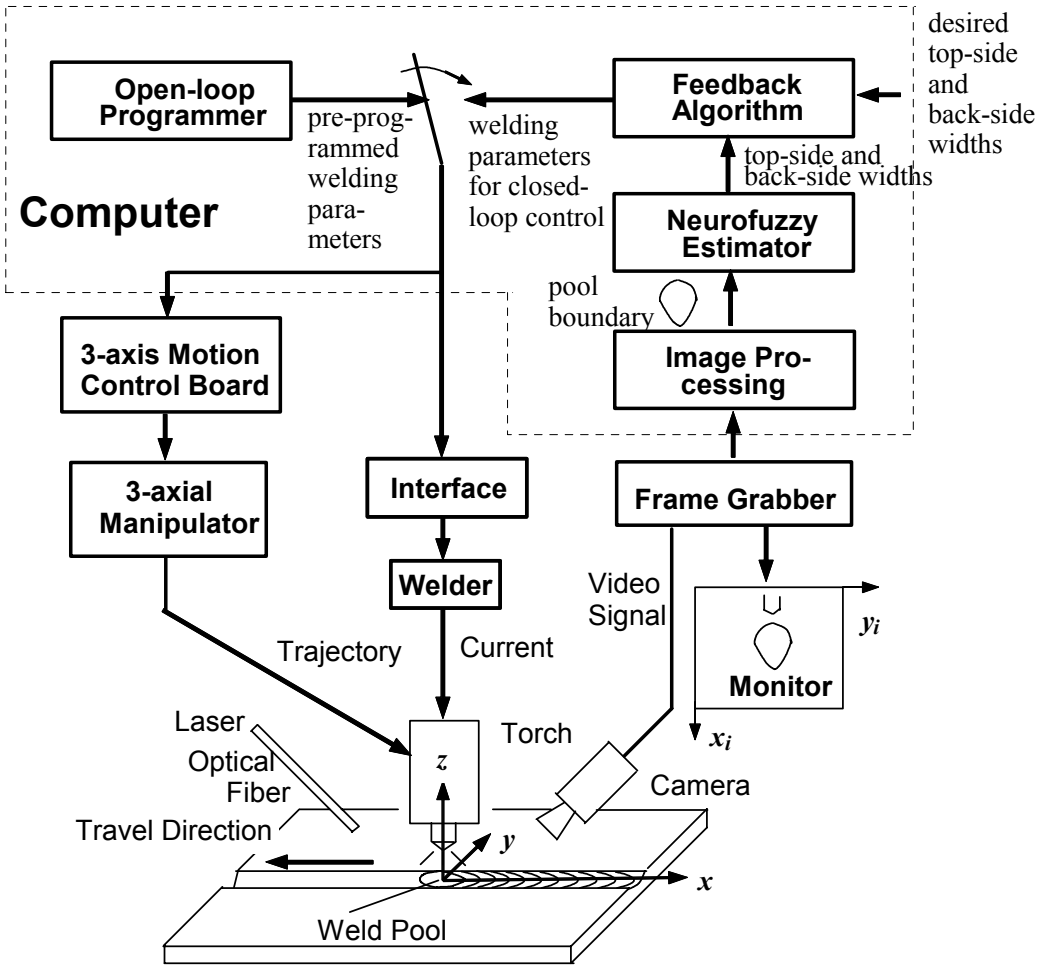

Fig. 3 Experimental setup

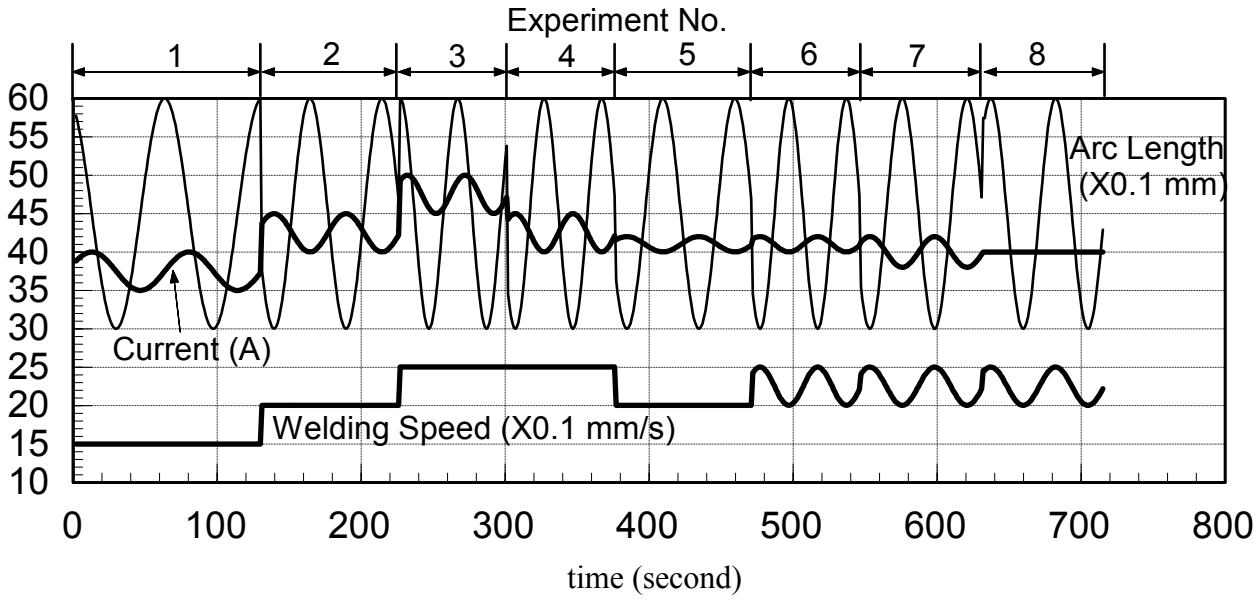

Fig. 4 Experimental inputs.

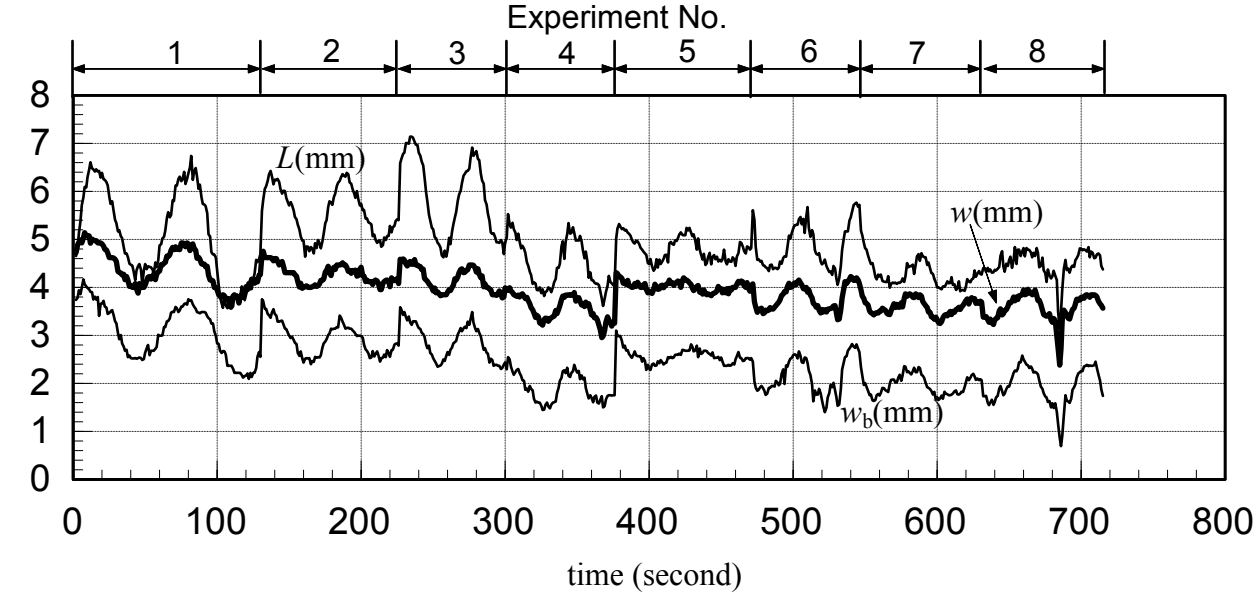

Fig. 5 Experimental outputs.

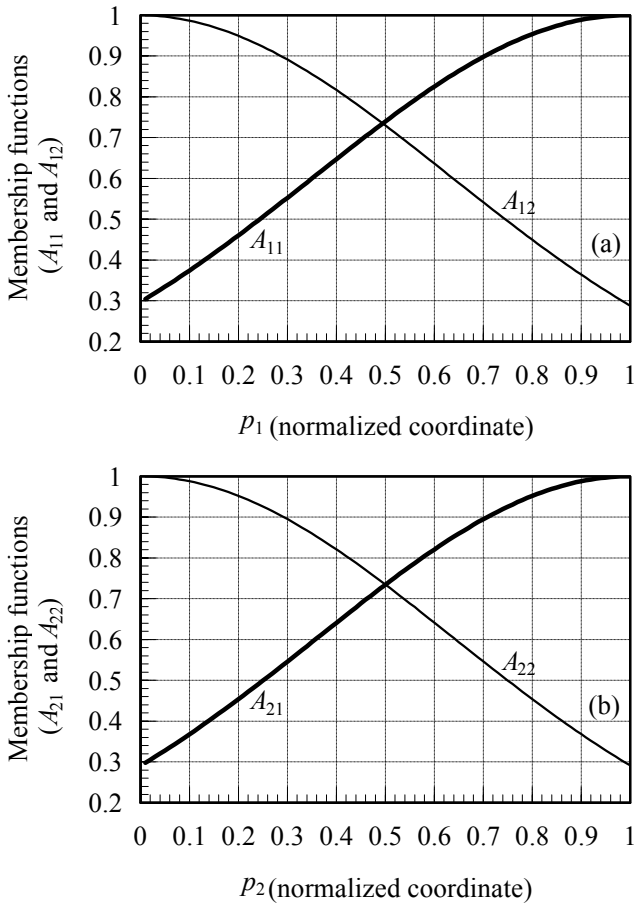

Fig. 6 Fuzzy membership functions. (a) Length partition. (b) Narrowness partition.

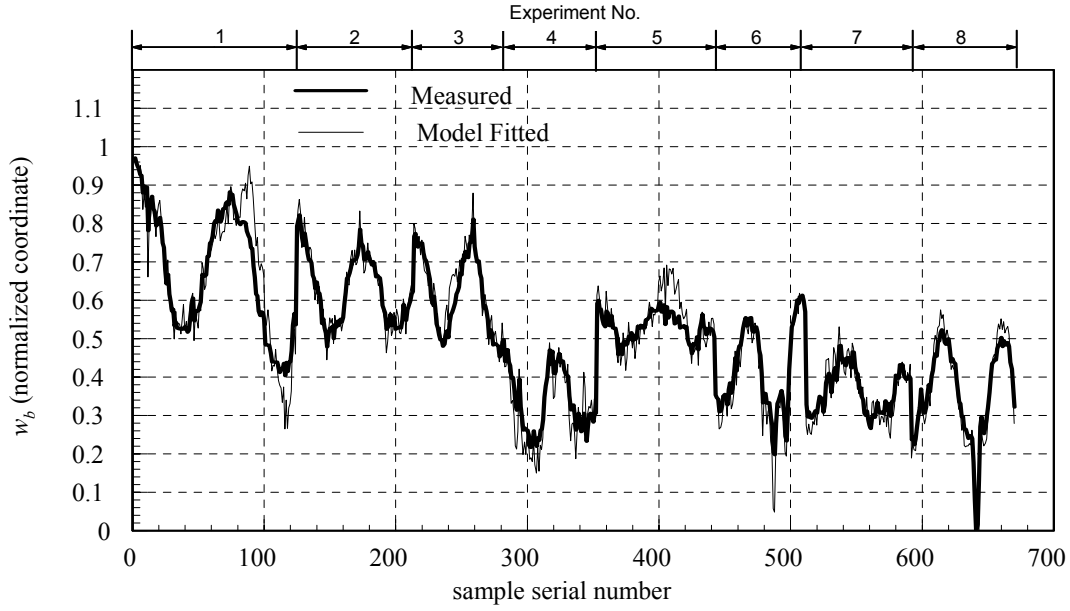

Fig. 7 Neurofuzzy fitting of the back-side bead width.

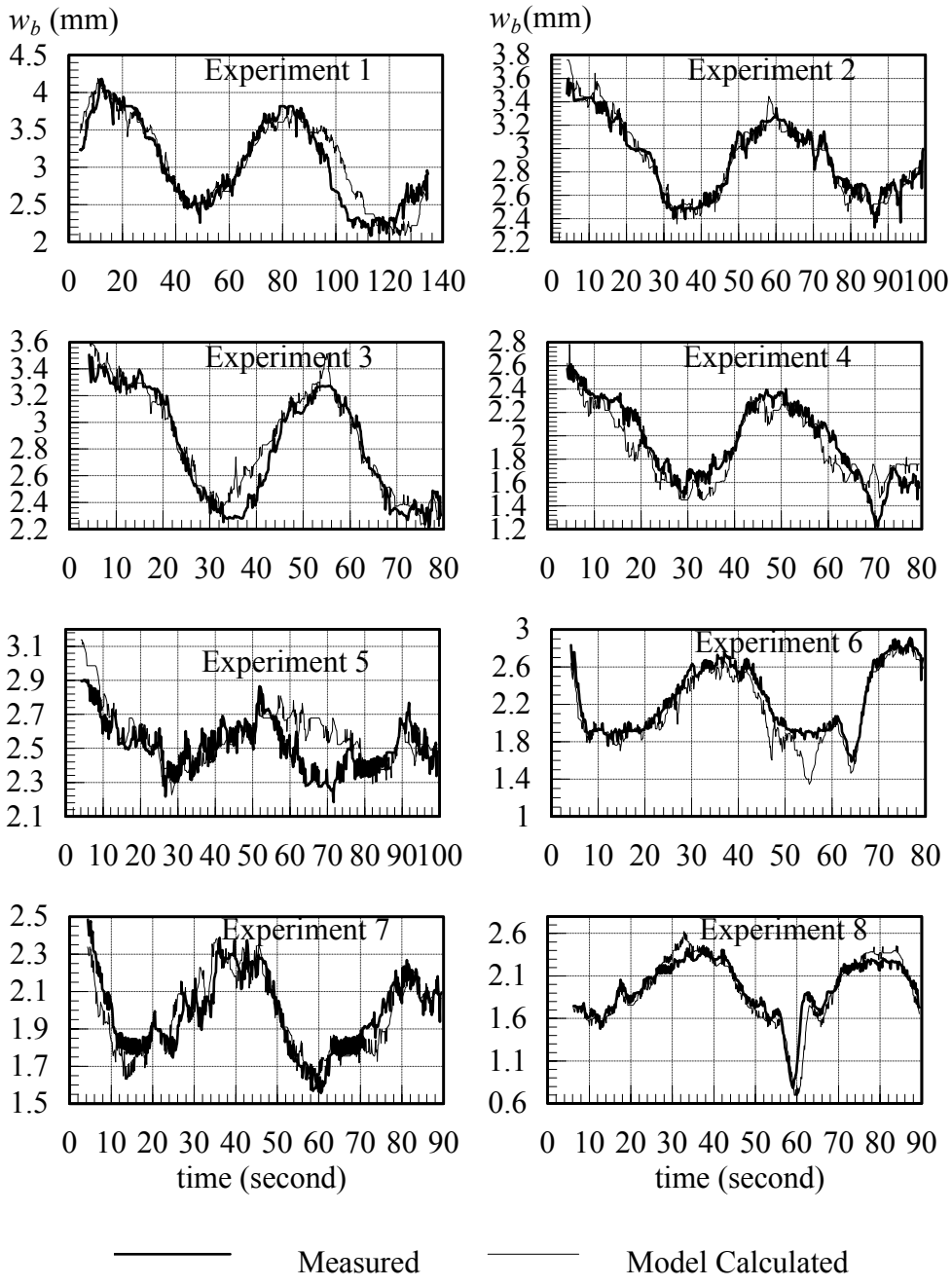

Fig. 8 Neurofuzzy prediction of w_b.

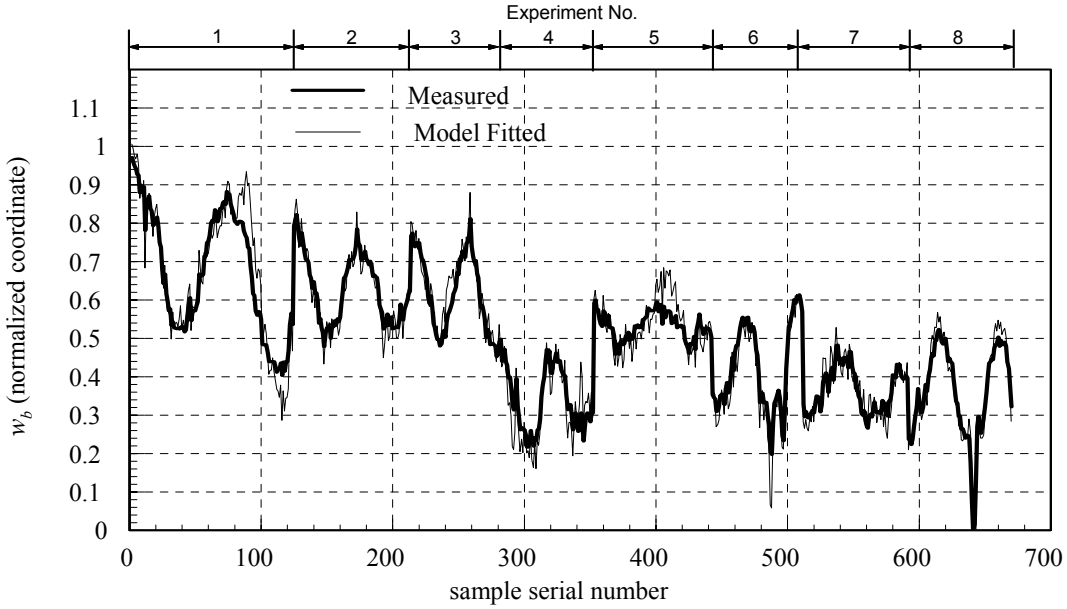

Fig. 9 Neurofuzzy fitting of the back-side bead width using $(I_1 = 3,\ I_2 = 3)$.

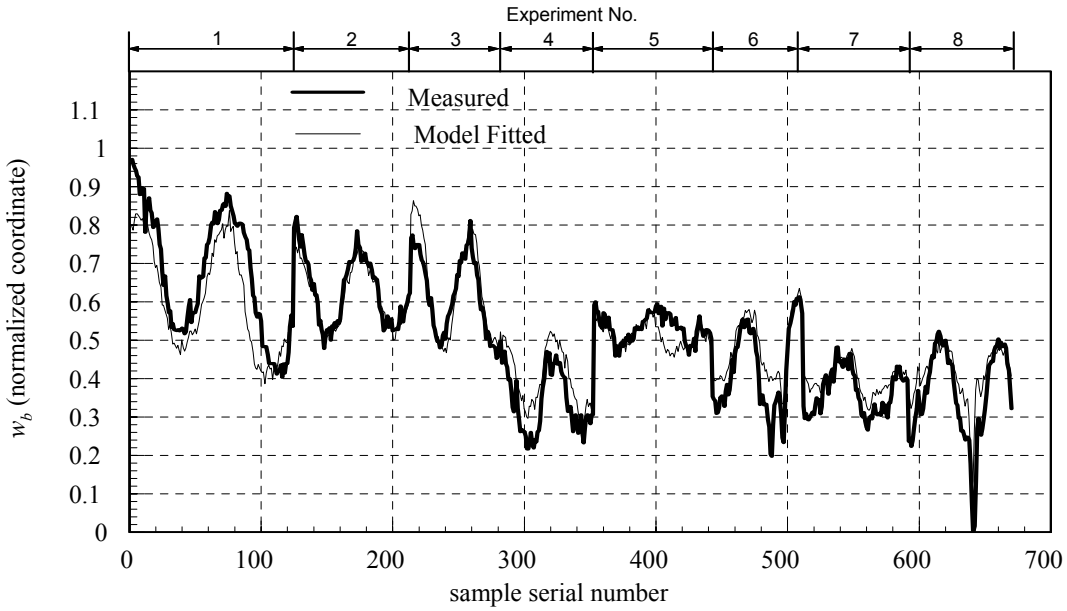

Fig. 10 Linear fitting of the back-side bead width.

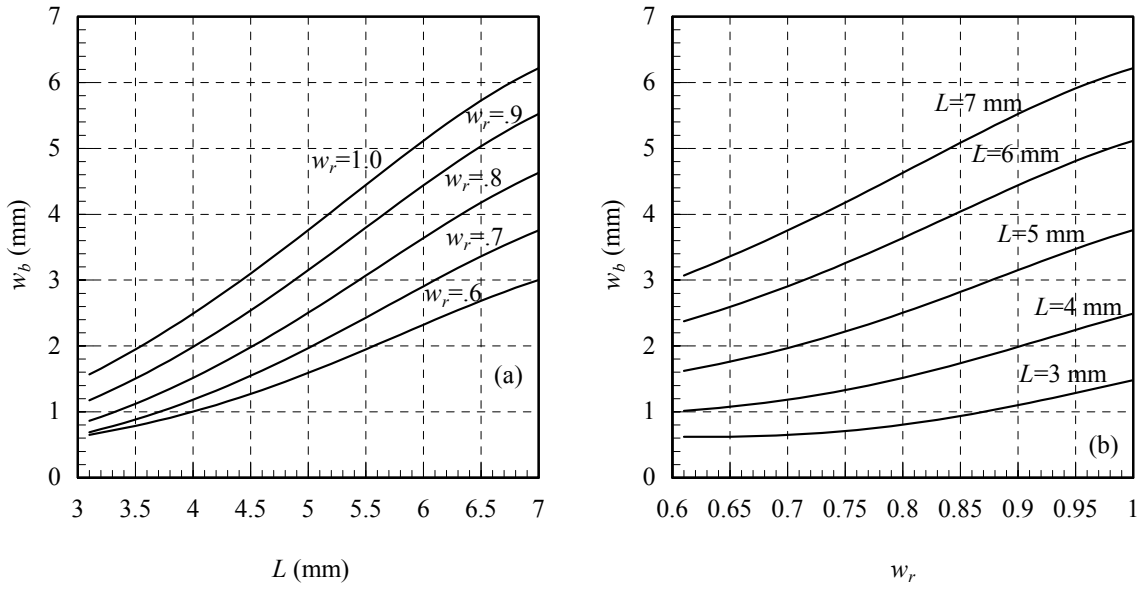

Fig. 11 Parametric curves of the neurofuzzy model. (a) $w_b \sim L$. (b) $w_b \sim w_r$.

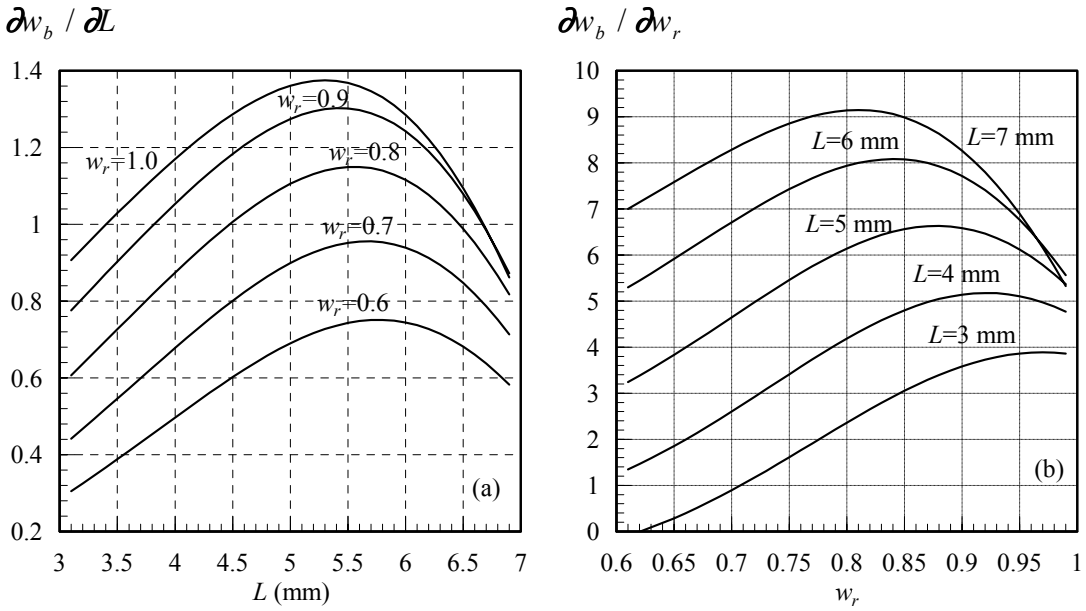

Fig. 12 Partial derivatives of neurofuzzy model predicted w_b. (a) $\partial w_b / \partial L$. (b) $\partial w_b / \partial w_r$.

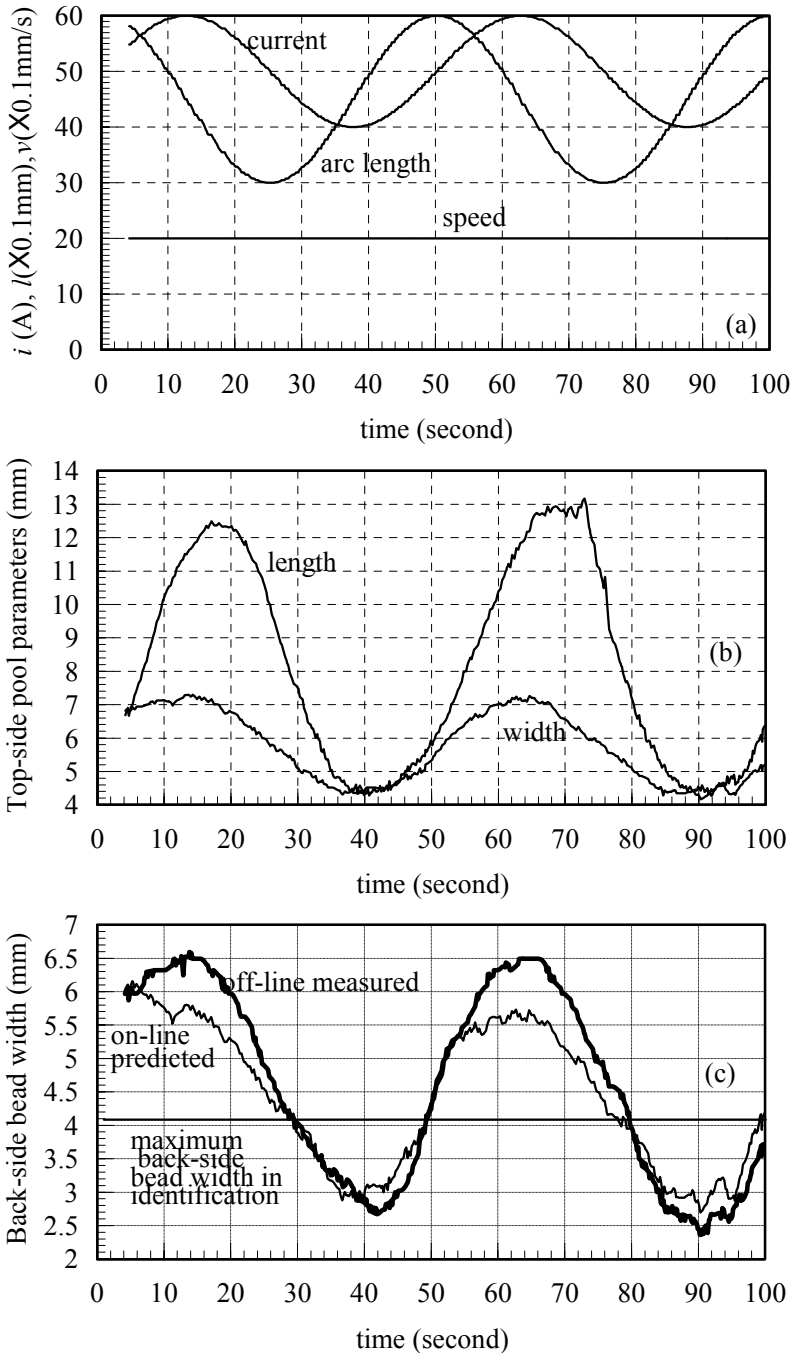

Fig. 13 On-line prediction experiment 1. (a) Welding parameters. (b) Top-side parameters of weld pool. (c) Back-side bead widths.

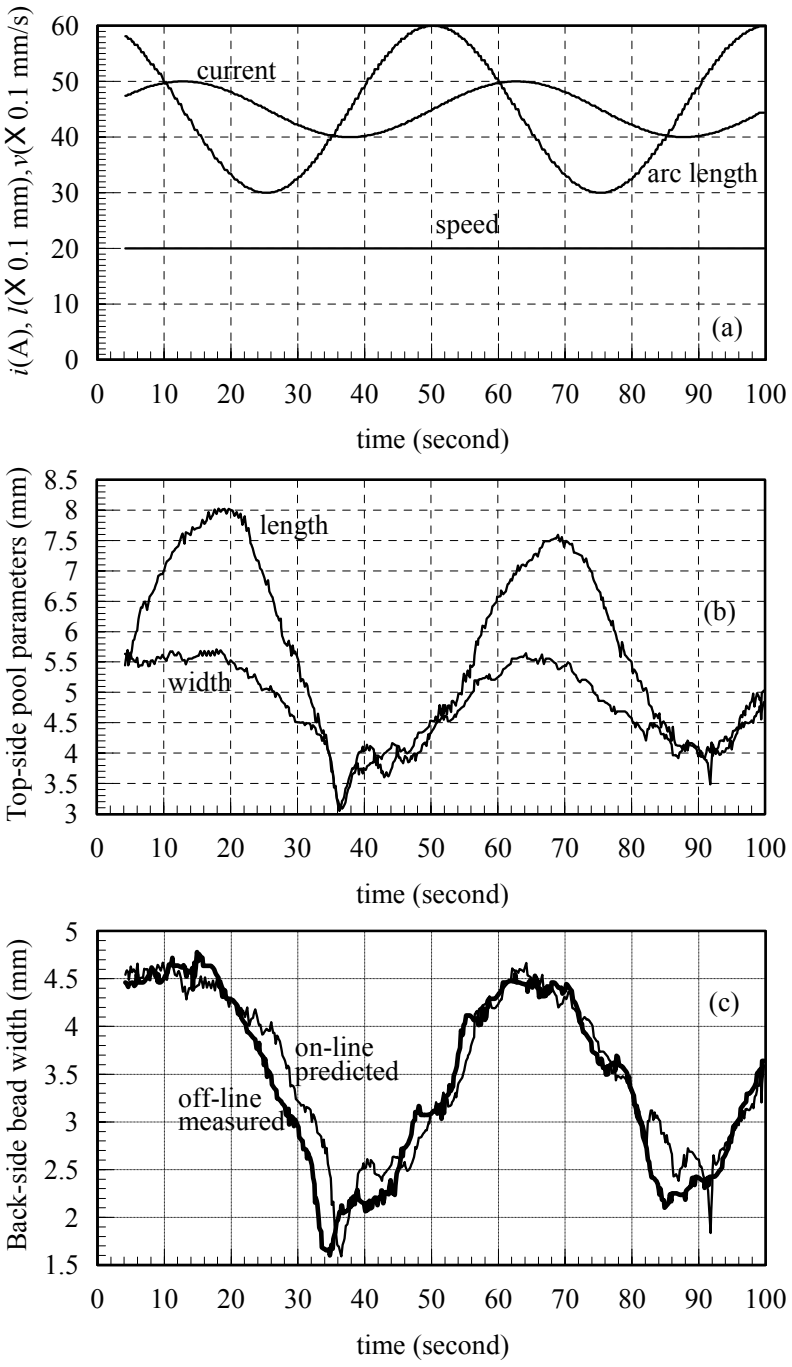

Fig. 14 On-line prediction experiment 2. (a) Welding parameters. (b) Top-side parameters of weld pool. (c) Back-side bead widths.